**Proceedings of the American Academy of Arts and Sciences.**

Vol. 64. No. 9.—August, 1930.

---

# THE JOULE-THOMSON EFFECT IN AIR.
## SECOND PAPER.

By J. R. Roebuck.

# THE JOULE-THOMSON EFFECT IN AIR. SECOND PAPER.

By J. R. Roebuck.

TABLE OF CONTENTS.



## 1. Introduction.

In an earlier paper[1] I have described the experimental set-up and detailed the results of the measurements on air at temperatures

---

A number of errors and misprints in the first Article[1] should be corrected as follows:

pp. 563–564, Tables I, Flow L/min. to Flow L/sec.
568–573, Tables II–IX, Flow L/min. to Flow L/sec.
568, second paragraph, line 5, minute to second
585, Table XI, Column 5, row 6, 0.0800 to 0.0700
589, Table XV, Column 2, row 3, 272.12 to 272.42
594, Fig. 15, On lowest Curve, 200° C to 250° C.

above that of the room. In the present article the data are extended to cover the available range below room temperatures.

The apparatus and procedure are essentially those described in the earlier paper, so that here it will be necessary only to describe modifications of apparatus and procedure required by the different conditions or suggested by more extended experience.

The steady growth in complexity of the apparatus over the years while this problem has been studied finally made it virtually impossible —or at least impracticable—for one worker to run the outfit and collect the data; consequently J. H. Webb joined me in the work and all of the data here presented, as well as some of the calculations, are the result of our joint effort. Upon J. H. Webb's departure, Harold Osterberg joined me and some of the calculations toward the end of this article are his work.

## 2. Thermostat Bath Arrangements.

For temperatures running down to $-150°$ C. it is necessary to use a variety of bath liquids, going to the more expensive materials only as necessity arises. Good kerosene serves for temperatures to perhaps $-50°$ C., but is apt to become viscous and is better changed to gasoline after $-25°$ C. The highest grade of gasoline could be used to about $-80°$ C. Petrolic ether (benzin petroleum) could be used to $-120°$ C. while below this isopentane[2] served to $-150°$ C. The cost increases in this order, but in no case was serious for the 4 gallons necessary to fill the bath. Several times liquids were used when their increased viscosity or partial solidification made them unsuitable. The performance of the apparatus and the vagaries of the data showed it unmistakably.

## 3. Bath Refrigeration.

For the runs at $0°$ and $-25°$ only, the coil in the lower part of the bath (See First Paper, Fig. 1) was rotated to new openings, connected outside to the carbon dioxide refrigeration system, and the apparatus was cooled by its normal use. The compressed condensed gas was brought to the expansion coil through a pipe enclosed in the larger pipe carrying the expanded evaporated gas back to the compressor.

For bath temperatures from $-50$ to $-150°$ C., the cooling was done by air exactly as in an air liquefier. The general flow diagram for the whole set-up is given in Fig. 1. The air compressed to 215 atm. from either or both compressors (1) and (2) passes through the trap

(3) for the separation of the liquid water, and through the drier (4) filled with stick sodium hydrate, which also serves to remove any carbon dioxide. Here (5) the air flow divides, part being used for cooling and part for passage through the plug. The portion to be used for cooling passes through the tubing of the short exchanger (6), the carbon dioxide boiler (7), and the long exchanger (8), expands to about one atmosphere at the valve (9) into the coil of tubing (10) which is welded to the outside of the steel cylinder forming the thermostat tank. It passes back from here through the exchangers (8) and (6) to the intake of the compressors.

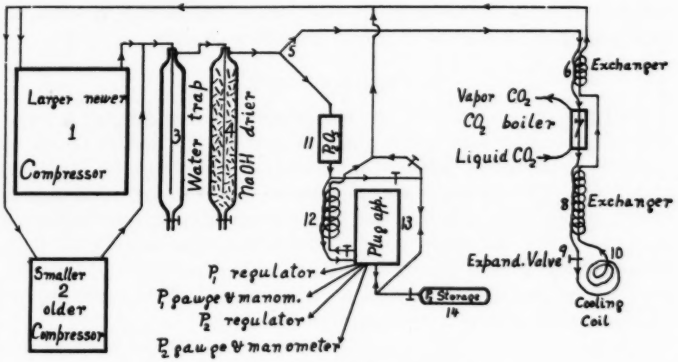


FIGURE 1. Flow diagram.

These exchanger coils are new and were constructed as follows—The coil of (8) was made of four pieces of copper tubing each 50 ft. long, $\frac{3}{16}''$ o.d., $\frac{1}{8}''$ i.d., wound in parallel to form flat "pancake" coils so that each pipe always progressed axially in one direction. The method of doing the winding is new and will be described elsewhere. The coil was carried on a $\frac{5}{8}''$ diam. spindle and slipped into a 3" i.d. brass tube. This brass case was later changed to red fiber with metal ends and the increased speed and range of cooling was very noticeable and valuable.

The smaller coil (6) was made of one piece of copper tubing 40 ft. long, $\frac{1}{4}''$ o.d., $\frac{3}{16}''$ i.d., wound like coil (8) in flat "pancakes." The joints required in the tubing were all made by cutting long male and female cones on the tube ends and fastening them together with a

minimum of silver solder. Such joints do not modify either inside or outside diameter of the tube, and they bend on the form almost as readily as the rest of the tube. Failure of the silver solder to make a tight joint is very unusual.

The rate of cooling so obtainable varied from 1.4° C. per minute at room temperature to 0.4° C. per minute when the bath was at −150° C. The total time required to cool down to the working temperature was as a maximum about 3 hours. The air coming from the caustic soda drier still carries a trifle of moisture. From −10° to −70° C. this kept clogging the expansion valve, so requiring much attention, but at lower temperatures this ceased, probably due to the deposition of the moisture on the walls of the tubing, whereas at higher temperatures some of it may have formed snow.

### 4. Plug Air Supply.

The part at (5) Fig. 1 of the compressed air destined for passage through the plug passes first through four or five inches depth of phosphorus pentoxide powder contained in a steel (11) tube 3½″ o.d. and 3″ i.d. This at times packed down so that it took several atmospheres to force air through, but the pressure drop was of negligible moment unless the oxide powder had been deliberately packed in filling. From here it passes to the old exchanger (12) and into the plug apparatus (13). It returns over the outside of the pipes of (12) and enters the return to the compressors' intake.

### 5. Thermometers.

As indicating instruments a mercury thermometer of range 0° to −28° scaled in $\frac{1}{10}$°, and a pentane thermometer of range 0° to −200° C. scaled in 1°, served somewhat to follow the bath temperature. The control mechanism could also be relied on both for actual temperature and for variations. The ultimate reference however was always the inlet thermometer.

The same pair of platinum resistance thermometers and the same auxiliary apparatus were used throughout this work as for the latter part of the work reported in the first paper.[1] Since the Callendar formula cannot be used below about −40° C. the general method described by Van Dusen,[3] by Loomis and Walters,[4] and by Henning[5] was used. The oxygen boiling temperature was chosen as the required extra point having the value −183° C. at 76 cm. Hg given by Van Dusen.

The oxygen hypsometer arrangement is shown in diagram Fig. 2. The oxygen was made by heating pure potassium permanganate

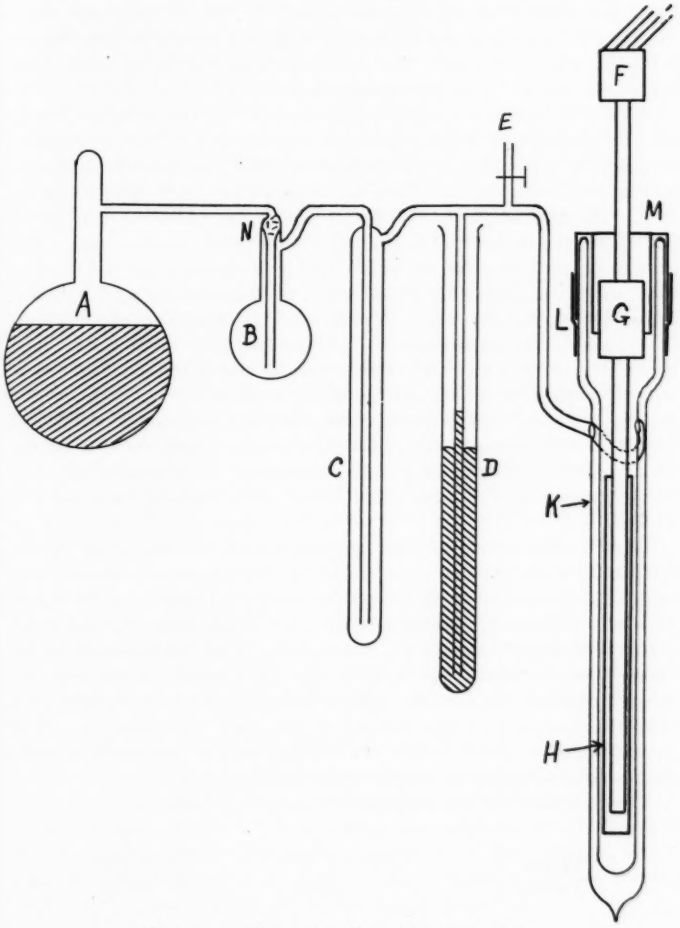


FIGURE 2. Oxygen boiling point apparatus.

in a large pyrex glass flask $A$. A certain amount of dust was carried over which was caught almost completely by an asbestos plug, $N$. The water carried over was partly condensed in the first trap, $B$, while the residue was largely condensed by the ice salt bath, surrounding $C$. The final residue was not sufficient to clog the tube where it first became very cold. The apparatus was thoroughly evacuated through $E$ before the permanganate was heated.

In their normal use a heavy metal head, $G$, on the thermometer is used for fastening it in the apparatus, and hence is held at a temperature usually not far from the temperature being measured. It therefore seems best to cool this head down to the oxygen boiling temperature. The final form of hypsometer used is that shown. The pyrex glass parts are shown by thinner and the metal by heavier lines. The oxygen passes across the vacuum space in $K$ through the coiled glass tube and is condensed by liquid air in the re-entrant metal cup, $M$, whose upper edge extends over and down the outside of the vacuum vessel where it is made tight by a rubber sleeve, $L$. The safety tube thrust into the mercury well, $D$, allowed the use of pressures considerably over one atmosphere during this condensation which proceeded rapidly and easily without overheating the pyrex flask. The liquified oxygen flowed down in contact with the case about the coil of the thermometer. A cylinder of thin aluminum, $H$, which fitted close to the glass served as a radiation shield. The vacuum tube was not silvered.

When sufficient oxygen had been collected, the liquid air in the re-entrant metal cup was replaced by liquid oxygen made from ordinary commercial oxygen, and the mercury lowered in the safety tube until the system was open to the air. Under these circumstances the liquid oxygen boiled away too rapidly to give confidence in the thermometer reading. To control this the vacuum vessel was immersed in liquid air and the oxygen boiled as slowly as desired by a small heating coil in the bottom of the tube (not shown). With everything thus under control the settings became as steady as could be desired and could be satisfactorily duplicated.

The constants for the thermometers are as follows:—

| | $\delta$ | $\beta$ |
|---|---|---|
| Therm. $X$ | 1.50 | 0.111 |
| Therm. $Y$ | 1.49 | 0.127 |

where

$$t = Pt + \delta\left(\frac{t}{100} - 1\right)\frac{t}{100} + \beta\left(\frac{t}{100} - 1\right)\left(\frac{t}{100}\right)^3$$

The data so obtained was used to plot a curve of corrections $(t-Pt)$ against $Pt$, for each thermometer which was used to make the correction direct from bridge reading to final corrected reading.

In this low temperature work it was difficult to check the difference in resistance of the thermometers at each working temperature. It is less here than at the higher temperatures since the difference falls steadily with the temperature, amounting to only 0.4° C. at −150° C. and also the observed $\Delta T$ is usually large. This difference when measured always agreed with the calculated value over the whole range of temperature to well within the limit required by the other errors. This experimental comparison was made at only a few points in the low temperature range.

### 6. Compressor.

The two-stage water-lubricated compressor used throughout the earlier work[1] was supplemented here by a three-stage water-lubricated compressor of 60 cu. ft./min. of free air actual capacity, built by the Nordberg Manufacturing Co., Milwaukee. During the preliminary cooling down of the bath both compressors were often used, see Fig. 1. Most of the readings were made with air handled by the larger machine since, on account of the lower temperature, the volumes to be handled in the plug were not so large and the mass flow could therefore be increased materially before kinetic energy effects became appreciable. These larger flows reduce the errors due to heat leakage which were larger in this range on account of the generally larger temperature drops measured. The large compressor was however not so steady in its delivery as the other had become and required a great deal of mechanical attention, particularly to the valves. The replacement of the castor oil by water on the piston rod of the small machine finally abolished the use of oil of any kind in the compressed air system, leaving only water vapor as the main impurity.

### 7. Pressure Regulation—Barostats.

The high pressure was controlled by the same barostat as used in the latter part of the earlier work. Its steady preformance is of dominant importance in determining the consistency of the data obtained. The single door-spring attached to the rotating piston load was used for all this work. An extended discussion of this regulator will be found in the earlier paper[1] page 549.

The most continual and persistent difficulty found in this work

was the slow shift of the pressure ($P_2$) inside the plug. This was attributed to clogging or unclogging of the plug by condensible material carried by the compressed air, and led to extreme measures to purify the air. The air from the sodium hydrate purifiers, see Fig. 1, was passed through phosphorus pentoxide powder held in a steel tube requiring 0.5–7 atmospheres to force it through. This improved the situation but did not cure it, so it was inferred that substances other than water vapor caused the trouble. The air approaching the plug bath was next passed through a long regenerator built after the Linde model of a casing steel tube and five internal copper tubes. The end where the air turned back on itself was immersed in liquid air, so that as determined by thermocouples along the tube, the flowing air actually approached liquid air temperature. This should effectively condense out any volatile material. While it again improved the situation, it still left $P_2$ varying too much for satisfactory data. Filtering the air while at this low temperature through cotton to take out snow made no observable difference. This, combined with the failure of many other less extreme measures, made the situation look almost hopeless after some two years of effort. But now the drift was small, usually, so it was decided to try keeping $P_2$ steady by direct regulation in the hope that the clogging was small enough to allow of satisfactory data.

For the control of $P_2$ a second rotating piston (see Fig. 4 of earlier paper)[1] was set up and used to operate a valve just as for $P_1$. A number of arrangements were tried and the most satisfactory was to make this control valve the one in the base of the apparatus through which the air escaped from the plug cavity. A second valve in the base in series with the controlled one, allowed of adjusting the division of pressure drop, so that any desired fraction could be left across the controlled valve. The fraction used was made small enough so that the tendency to hunt was kept within manageable dimensions. A wooden cylinder about four inches in diameter was used on the valve stem to reduce its angular motion as compared with the sliding contact motion, and the motor speed was reduced 96:1 by a worm gear and 4:1 by pulleys. By control of the voltage applied to the 20 volt D.C. motor the overshooting was readily controlled and it was found best to set it so that the motor was in continual motion, and the valve oscillating through a very small angle on each side of the steady setting.

The volume capacity of the plug and passages is small, so an ordin-

ary carbon dioxide storage cylinder, 25 lb. size (see 14 of Fig. 1) was connected to it, and provided with filling and emptying connections direct to the high and low pressure lines in order to economize on the time required for shifting the working pressure.

All this, together with the spring on the rotating cylinder, made the control of this pressure exceed expectations. The situation is much simpler than with $P_1$, since $P_2$ is not subject to any erratic rapid variation. The tendency to hunt was under entire control. At a shift in the working pressure, the new pressure became steady immediately and remained so with very little attention. The piston shifts vertically while compensating valve temperature adjustments and possibly some plug clogging, but this lasts only a short time after each shift.

The effect on the data was apparent from the first. The difference of temperature reading settled down immediately to its final value; that is, generally within 5 minutes after setting at a new pressure difference, the temperature difference was steady and would keep the same value to 0.01° for as long as it was followed (30 minutes in one case).

It appears from these observations that the flow varied but very little, particularly at the lowest bath temperatures. The observed drift of the uncontrolled $P_2$ must therefore be sought elsewhere than from impurities, as for instance in the temperature shift of the valve stem and parts about the valve.

## 8. General Theory. Thermodynamics.

The porous plug (Joule-Thomson) and the free (Joule or unresisted) expansion experiments belong to that large class of problems in the consideration of which the forms of energy entering the discussion may be restricted to two, heat and work; and the transfers of work may be restricted to those accomplished by a uniform hydrostatic pressure. In such cases it is generally observed that there are only two free variables. On the basis of the conservation of energy, one may write

$$du = dq - pdv$$

where $u$ is the intrinsic energy and $q$ the heat added. Also

$$dq = CdT + h'dp$$

which is the definition of $C$* and $h'$. Whence

$$du = CdT + h'dp - pdv$$

* Since $C_v$ is not used here, $C$ is used for $C_p$.

One of the Maxwell relationships (the first) is

$$h' = -\,T\left(\frac{dv}{dT}\right)_p$$

from which

$$du = CdT - T\left(\frac{dv}{dT}\right)_p dp - pdv \tag{1}$$

which except for the $u$ involves only quantities quite familiar in the laboratory, and is readily applied to the expansion experiments being considered.

In the *porous plug* experiment, the system is insulated from heat exchanges but not from work transfers, so that the condition to be satisfied is

$$u + pv = h = \text{constant}$$

and imposing this condition on the general equation (1) gives very easily the well known equation

$$C\mu = C\left(\frac{dT}{dp}\right)_h = T\left(\frac{dv}{dT}\right)_p - v \tag{2}$$

In the *free expansion* experiment, the system is isolated and neither work nor heat may be transferred across the boundary. That is, the energy of the system remains constant, or

$$u = \text{constant}$$

Imposing this condition on Eq. (1) gives

$$C\eta = C\left(\frac{dT}{dp}\right)_u = \left[T\left(\frac{dv}{dT}\right)_p - v\right] + \left(\frac{d(pv)}{dp}\right)_u \tag{3}$$

or

$$C\eta = C\mu + \left(\frac{d(pv)}{dp}\right)_u \tag{4}$$

which is a very simple relationship between the two coefficients $\eta$ and $\mu$. It is a precise statement of the readily recognized experimental situation, namely that the difference between the porous plug and the free expansion situations is the external work factor. It says that for unit change of pressure ($dp$) the quantity of heat ($CdT_u$) required to keep the temperature ($T$) constant in the free expansion experiment is equal to the heat ($CdT_h$) required in the similar porous plug expansion experiment, plus the heat $\left(\frac{d(pv)}{J}\right)_u$ equivalent to the change of $pv$ in the free expansion experiment.

While Eq. (2) may evidently be used for computing $\mu$, it is not very serviceable, since the term $\left[ T\left(\frac{dv}{dT}\right)_p - v \right]$ is a small difference between larger experimental quantities. This applies also in Eq. (3) and moreover the variation of $C$ with temperature and pressure has not been measured at all adequately. Conversely, if $\mu$ be known experimentally it offers an excellent method for calculating either $\left(\frac{dv}{dT}\right)_p$ or $v$.

Eq. (4) may readily be put in a form very suitable for computation, using the data for $\mu$. Since there are only two free variables, if $(pv)$ be chosen as a dependent variable, one can write

$$d(pv) = \left(\frac{d(pv)}{dp}\right)_T dp + \left(\frac{d(pv)}{dT}\right)_p dT \tag{5}$$

which holds generally and will therefore hold for the free expansion experiment where $u$ = constant, or

$$\left(\frac{d(pv)}{dp}\right)_u = \left(\frac{d(pv)}{dp}\right)_T + \eta_i \left(\frac{d(pv)}{dT}\right)_p \tag{6}$$

and substituting this in (4) gives

$$\eta_i \left[ C - \left(\frac{d(pv)}{dT}\right)_p \right] = C\mu + \left(\frac{d(pv)}{dp}\right)_T \tag{7}$$

The variation of $(pv)$ as a function of $p$ and of $T$ is a very common way of expressing the properties of a gas. Such tabulations may readily be used to supply these two partial differential coefficients, and with $C$ spread over the pressure range by the use of the isenthalpic curves (see first paper[1]), $\eta_i$ may be readily calculated. Moreover, if one carries out the indicated differentiation (7) yields

$$\eta_i \left[ C - p\left(\frac{dv}{dT}\right)_p \right] = C\mu + p\left(\frac{dv}{dp}\right)_T + v \tag{8}$$

in which however the second and third terms on the right give again the small difference between larger experimental quantities.

Also if in (8) one substitutes the values of $\mu C$ from (2), there results

$$\eta_i \left[ C - p\left(\frac{dv}{dT}\right)_p \right] = T\left(\frac{dv}{dT}\right)_p + p\left(\frac{dv}{dp}\right)_T \tag{9}$$

It might be observed that it is not required in this argument that the system be homogeneous, that is, of one phase only, though the physical meaning of the coefficients may differ in the two cases. This situation arises, for example, in this work where the isenthalpic curves cross the vapor pressure area of a several component system.

## 9. Experimental Results, Isenthalps.

The data from the experiments are given in Tables 1–12. The separate Tables are referred to by the approximate bath temperature. In each Table the data is grouped under letters to indicate the group readings (runs) made at one attempt. The last reading of the temperature and pressure in a run (numbered serially) is the bath temperature and the inlet high pressure. The temperatures are all reduced to the hydrogen Centigrade scale. The pressures are all in atmospheres (76 cm. mercury at 0° C.) and are in absolute terms, that is above zero not above atmospheric. The plug used is referred to by number. In general all the data are in duplicate agreeing with each other and taken with a different plug and rate of flow in the separate runs. The rate of flow is not given and was generally not recorded, care being merely taken to insure that the rates were different and neither excessively large or small. Each run has a particular plotting symbol so that the points may be distinguished on the plot.

The data are plotted in Fig. 3 using an unbroken pressure scale as abscissa but a temperature scale as ordinate with gaps in the scale to economize in the area needed. This shifts the curves out of their natural relation to each other and account must be taken of it when making comparisons. Reference to the earlier article will show immediately that the two series of curves fit together precisely—the change of position, of slope, and of curvature is regular and continuous. The growing steepness and curvature with falling temperature in the earlier work continues here, with maximum steepness at the lower end of the −85° C. curve approaching 1.6° C./atm. The curvature gradually concentrates towards the middle of the curve and increases so that while the lower end is still growing steeper, the upper end reverses its trend and grows flatter. The sharpened bend or knee moves down the curves until it fades out under and into the liquifaction curve. The data for this vapor pressure area as plotted in Fig. 3 are taken from the work of Kuenen and Clark[6] and of Dodge and Dunbar.[7] In the case of air, the

width of this saturation area is so small that any attempt to follow by experiment these isenthalpic curves within this area will be hardly profitable.

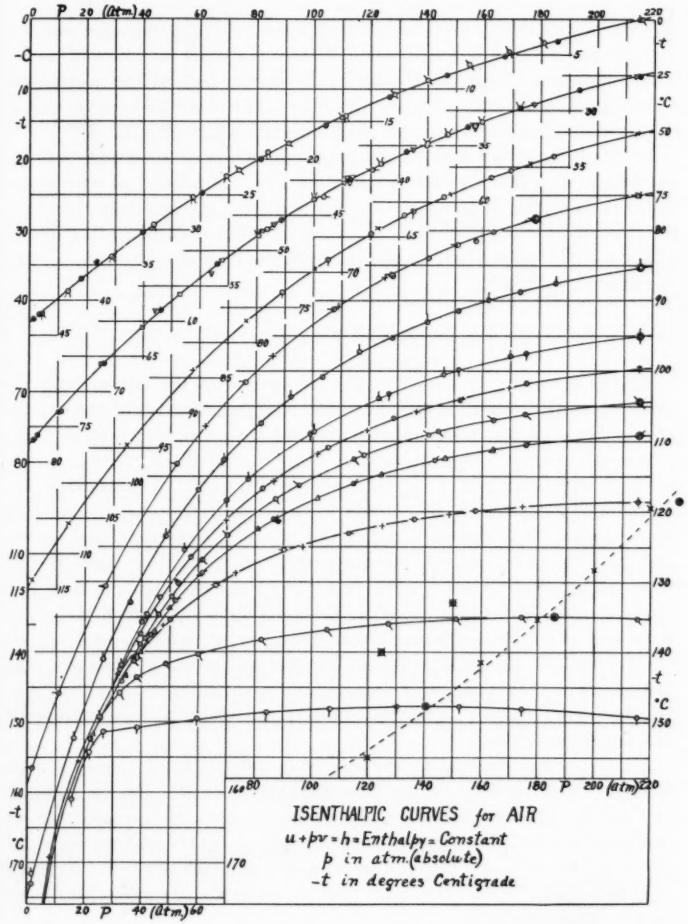


FIGURE 3.

It will be observed in Fig. 3 that the curves actually run into the saturation area, as they should, except in the lowest few points on the $-150°$ C. curve. These lowest two curves have only one run each—time failed at the close of the year. Also this $-150°$ C. curve was irregular in the way the equilibrium temperature was approached. It sometimes required half an hour before the drift had slowed down so as to be no longer observable while in the rest of the work five minutes was sufficient. This shows also in the $\mu$ for this curve which is the most irregular of all this lowest temperature group.

It should be noted also that the low end of the $-75°$ and $-85°$ C. curves are also determined by only one run. It proved so extremely difficult to avoid clogging of the plug with these large drops of temperature that when such curves as shown were obtained after many trials and the upper half or so was confirmed by another run, it was considered sufficient.

### 10. Locus of Maxima $\left(\frac{\Delta T}{\Delta P}\right)_h = \mu = 0$

The progressive flattening of the upper end of the curves, Fig. 3, proceeds until the sign of the slope reverses and on three of the curves the location of the maximum is marked by a cross surrounded by two small circles. The plot of $\mu$,—the slope of these curves, as described later—against $T$ at constant $p$ in Fig. 6 gives another set of points (put in with $x$) on this locus of maxima, and the dashed curve in Fig. 3 is drawn through the group. The other two points put in with circles over a cross are the data taken by Hausen and reported by Knoblauch.[8] The position of the maxima on such flat curves is very difficult to locate but the divergence between Hausen's data and these here is larger than the apparent experimental errors. On account of the care taken in the present work in pressure and temperature regulation and duplication with different rates of flow (in the other curves), the probabilities of error are less than with Hausen's procedure.

Fig. 4 is the same as in the earlier article[1] (Fig 11 there) except that the lower branch of the unnamed curve is now drawn through the points just determined. The general aspect of the situation as discussed in the earlier paper is not changed. The area enclosed by the loop as well as the probable maximum pressure is increased slightly. The whole area can still be explored experimentally by means now available.

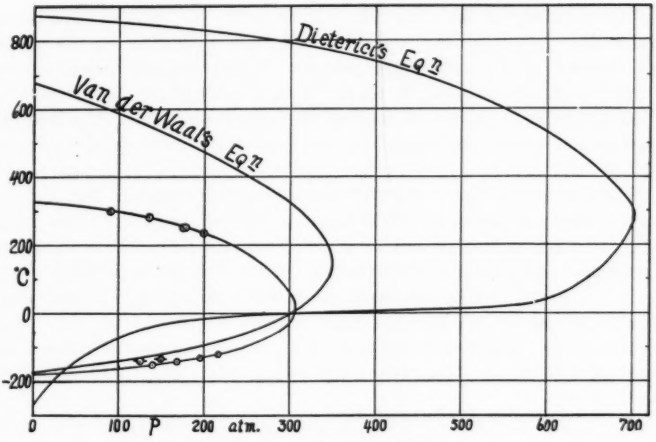


FIGURE 4. Loci of Maxima.

## 11. JOULE-THOMSON COEFFICIENT $\mu$.

As in the previous paper[1] the numerical values of $\mu$ are obtained by taking the ratio of successive differences of $t$ and $p$ for each run. These values of $\mu$ were then plotted against the average value of the pressure to give the set of curves of Fig. 5. They are plotted each to the same abscissa zero but the ordinate $\mu$ scale is broken to separate these curves. It will be observed that the curves shift both linearly and angularly, positively and negatively in each case, so that the normal plotting leads to inextricable confusion among curves and points.

Evidently while taking the first differential has increased the variation and consequent uncertainty, nevertheless the position of each of these curves is fixed within fairly narrow limits. To lessen the uncertainty as much as possible, the procedure described in the earlier work was again followed but even more thoroughly. The values of $\mu$ from the curves of Fig. 5 were used to reproduce the curves of Fig. 3. The position and curvature of the curves of $\mu$ were shifted slightly until they satisfied the criterion, that is, until by starting at a middle point of a curve of Fig. 3, a numerical integration of the values of $\mu$ reproduced the curve within the experimental error. This was a very long tedious numerical process but it added immensely

to the certainty of the $\mu$ curves. The 0° and −25° curves have much more data but it is less consistent than the following curves where the control of $P_2$ was improving due to better purification of the compressed air and finally to the actual control of $P_2$. It is also evident that this process of making the $\mu$ curve agree with the integral curves has in no case made the curve inconsistent with the plotted points.

The curves of Fig. 5 are still isenthalps like those in Fig. 3 from which they are derived. To change the data to isopiestics the value of $\mu$ for a set of integral values of $p$ were picked off and the values of $t$ corresponding to the $p$'s were read from Fig. 3. In Fig. 6 these values of $\mu$ are plotted as a function of $t$ at constant $p$. To complete the set of curves the corresponding values of $\mu$ and $t$ for the range above room temperature are included. Since the curves run so far along the $t$ axis the diagram is cut in two parts and these placed to save space.

It will be observed that the two groups of data merge with each other without any need for adjustment. The values also drop very excellently on smooth curves. At high temperatures the value of $\mu$ for all pressures is small, becoming negative for the highest pressures shown. The trend of the curves shows very definitely that $\mu$ will be negative for all these pressures at temperatures less than 100° C. above those shown. This agrees with the discussion on Fig. 4 above.

As the temperature falls $\mu$ increases with increasing rapidity for all pressures but the more strongly for the lower pressures. Within 100° C. of the critical temperature this increase of $\mu$ changes to a decrease, for the higher temperatures, giving flat maxima. As these maxima are followed to the lower pressures and consequent lower temperatures, they become sharper and sharper peaks until the curve suddenly fails to turn down and continues rising apparently indefinitely. The last maximum must be a sharp cusp, and the situation there is very peculiar both in the diagram and with respect to the physical state of the material.

Corresponding to the steepness at the maximum the left hand side falls with increasing steepness until apparently the critical pressure is reached. If these curves were for a single component (pure) material one could say confidently that for pressures below the critical pressure $\mu$ shows no maxima but continues to rise, as appears to be the case here.

The fall on the left of the maxima carries the values of $\mu$ down to

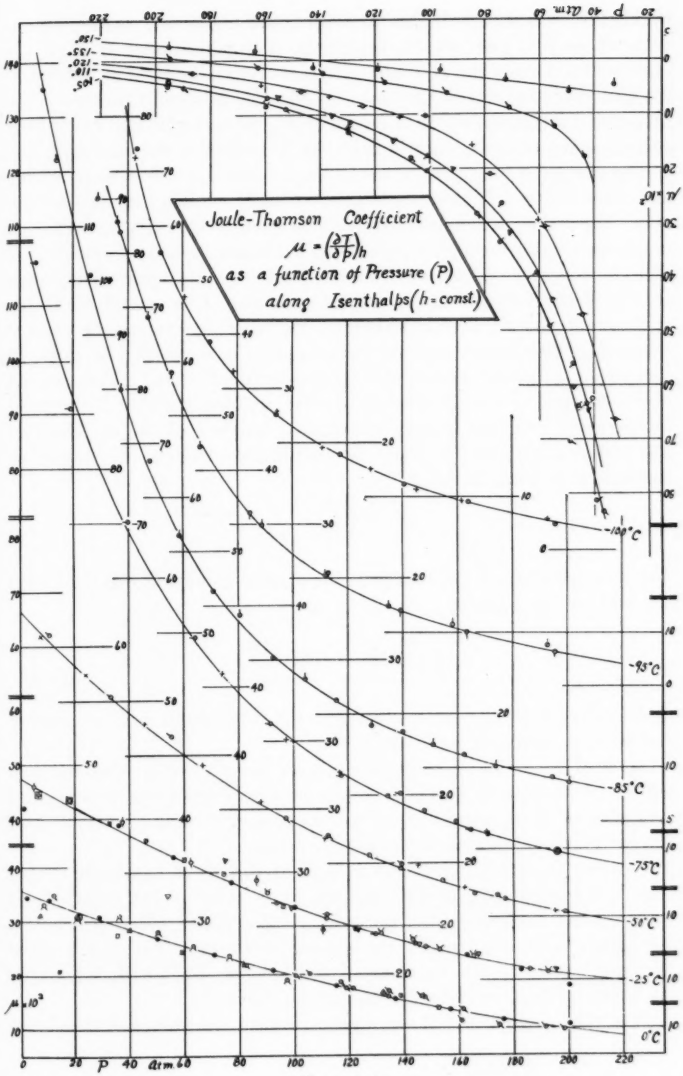
Joule-Thomson Coefficient
$\mu = \left(\frac{\partial T}{\partial p}\right)_h$
as a function of Pressure (P)
along Isenthalps (h = const.)
-100°C
-95°C
-85°C
-75°C
-50°C
-25°C
0°C
P atm.
$\mu \cdot 10^3$

FIGURE 5.

and below zero for the higher pressures, and unless the sudden curvature whose first part shows, interferes, it would appear as if all the curves would cross the zero line. This is of some interest as determining the lower branch of the curve of Fig. 4. It should preferably be attacked experimentally in the case of a pure material and one whose critical temperature is more easily reached, than is the case with air.

The curves of Fig. 3 run into the vapor pressure curve, some above and some below. If this vapor pressure curve was a line and not an area, then the isenthalpic curve which runs through the critical point should run through it parallel to the vapor pressure curve.[13, 14, 15] This of course is what one would expect from the general lay out. In Fig. 6 the value of $\mu_c$ ($p_c = 37.2$ atm. and $T_c = -140.6°$ C. for air[6]) should fall on the critical isopiestic where it crosses the critical temperature ordinate, and its value should agree with the slope of the vapor pressure curve, also at the critical state. The critical isopiestic runs so nearly vertical that its crossing point of the critical temperature ordinate is very uncertain. In view of the certainty of the above argument, it would be justifiable to draw this isopiestic through this point making

$$\mu_c = \left(\frac{dT_c}{dp_c}\right)_{v_c}$$

The average slope of the area near the critical condition was read from the plot of Fig. 3 giving

$$\left(\frac{dp_c}{dT_c}\right)_{v_c} = 0.63 \frac{\text{atm.}}{1° \text{ C}}$$

and the point is put in as $c$ on Fig. 6. This point falls almost on the 40 atm. isopiestic as drawn.

Air is of course not a single but a three component system, but one with a very narrow vapor pressure area and with the two critical points very close together,[6] so that it evidently makes a very good approximation to a one component system.

The fact that this point falls so high up on the $P_c$ isopiestic means that the greater part of the adjustment in slope of the isenthalpics between the gas region and the liquid region takes place just below the critical state and under the saturation curve. This takes place as noted above by the sharp bend sliding down the isenthalpic curve till it is cut off entirely by the saturation curve.

It is also evident that if one were to collect the values of the slopes

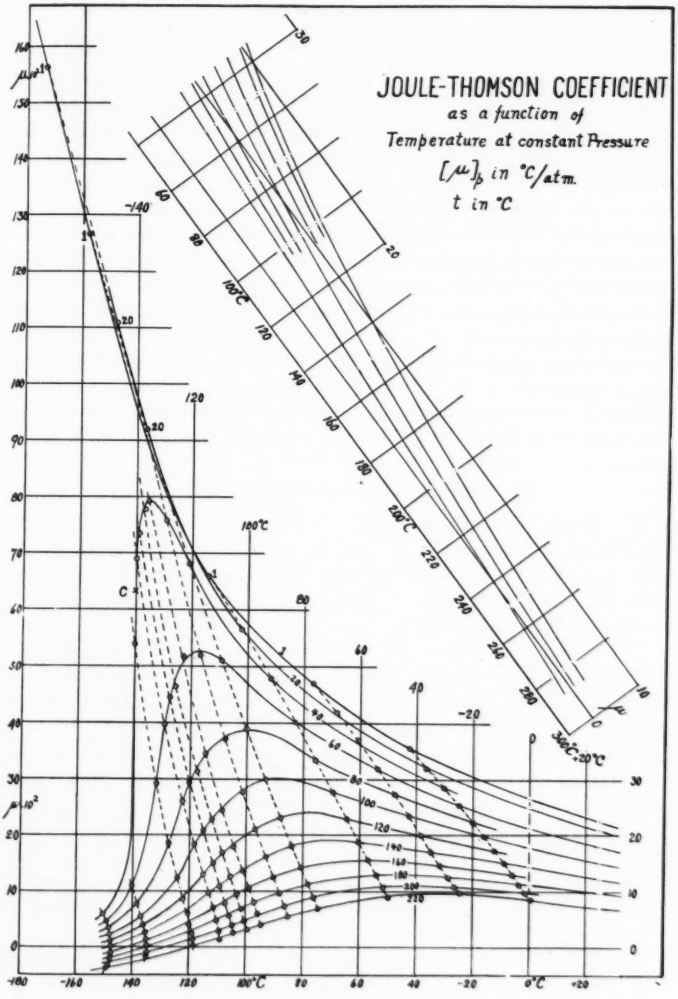
JOULE-THOMSON COEFFICIENT
as a function of
Temperature at constant Pressure
$[\mu]_p$ in °C/atm.
t in °C
100°C
200°C
300°C
0°C
-20°C

FIGURE 6.

of all the isenthalpic curves at the point where they cut the saturation curve (Fig. 3) these values would be the limiting values of $\mu$, maxima for these isenthalps on both the liquid and vapor sides. In the plot of $\mu$ against $T$ of Fig. 6, these values mark off an area which might be called the saturation area. At first it would appear as if none of the $\mu$ curves should cross this boundary, but it is to be observed that these plane diagrams are better considered as orthogonal projections from a three dimensional diagram in which the limit curve will be a line on the ($\mu$, $p$, $t$,) surface. There is no reason why this surface, carrying the isopiestic curves, should not dip below this limit (saturation) curve as it apparently does in Hausen's formulation[12] and here where the $p = 1$ isopiestic crosses that for $p = 20$ (see Fig. 6). Hence, in the projection, these isopiestics can and do invade the area inside this limit curve.

For further use the values of $\mu$ for a set of integral values of pressure and temperature were picked off the large plot and are collected in Table 13. They cover only the low temperature range and must be combined with Table XI of the first paper[1] to cover the whole range measured.

## 12. Comparison with Hausen's Work.

The group of workers, Vogel, Noell, and Hausen,[12] with Prof. Knoblauch at Munich have done the only comparable work in this field with air. They have all used the same general methods and even the same apparatus, so that only the final worker, Hausen's, results need concern us here.

To compare the values of $\mu$, the large scale plot of $\mu$ as a function of temperature at constant pressure, generously sent me by Hausen himself, was used to pick off the values of $\mu$ for 0, 100, and 200 atm. and the series of temperatures of the table, and are printed in italics in Table 14. The comparison values from the present work are printed in ordinary type. In parts of the field the agreement is excellent, about 1% near room pressure and temperature, but in other parts the difference goes in the extreme case to 300% for the small values. Even in the larger values the difference may amount to 50%. Since both groups of data have been smoothed to exclude as far as possible chance uncertainty of individual readings, there is not much purpose in a more detailed comparison than Table 14 affords.

In my first paper there is a discussion of the causes of uncertainty in Noell's work. Hausen used exactly the same plug arrangements. He calculates in some detail the heat leaks to be expected but he

gives no experimental verification, for example, that the readings are independent of the rate of flow. Nor does he consider seriously the effects of velocity of flow, nor the effects of drifts from the hand regulation of pressure and of temperature. Until something is known experimentally with his apparatus about these sources of difficulty, I am inclined to suspect the causes of the divergence lie there.

### 13. Specific Heat, $C = C_p$.

In the first paper, p. 586, the method of calculating $C$ was in error, in that the values of the factor for even values of temperature and pressure were picked off from the factor plot. This should have been done after the factors had been multiplied by the appropriate value of $C$ on the one atm. line. These values for $C$ have consequently been recalculated, but are substantially unaffected by a more correct smoothing.

To spread the values of $C$ over the pressure-temperature range, it is necessary to know a series of values of $C$ along a line cutting the isenthalpic curves of Fig. 3. Such a series of values would be sought first at $p = 1$ atm. over the temperature range. While this was excellent for the work above room temperature it is not very suitable for the present work, because, (1) a considerable portion of the curves do not extend to 1 atm. but end at the saturation curve, and (2) those curves which do extend to 1 atm. are widely spaced, run very steeply, and are perhaps the most uncertain experimentally. Above atmospheric pressure there are available Witkowski's[9] work up to 70 atm. and Jakob's[10] values calculated from the related properties of air. For the present purpose it would appear very profitable to use a method based on that used for water by H. L. Callendar[11] to measure the ratio of the specific heats at 100 atm. from room temperature to below the critical temperature.

Meanwhile the values given by Jacob[10] were used to calculate values of $C$ at 100 atm. down to a lowest temperature of $-80°$ C. The calculated values are given in Table 15, which includes the Table XII from the previous paper unchanged except for the value at $p = 100$, $t = 0°$ C. which is shifted from 0.2804 to 0.2838.

The curves are of some interest but can profitably await values of $C$ at such a pressure and temperatures as will serve to spread the values down to and below the critical temperature. Consideration of the curves of Fig. 3—whose meeting points mean a change of energy with no change of temperature or pressure—as well as the general

theory of the critical state, make $C = \infty$ at $T = T_c$, $p = p_c$. (Compare also Burnett [15, 16] and Hausen.[12]) The data of Table 15 show the very rapid rise of $C$ at the low temperatures, a rise which is different for each of the isopiestics.

### 14. Enthalpy $h$.

This quantity, $h$, is known by a variety of names—"intrinsic energy," "total heat," "thermodynamic potential," "$\chi$ function" (Gibbs)—as well as by a variety of symbols. The relation

$$[dh = Cdt]_p \quad \text{where} \quad C = \left(\frac{dq}{dt}\right)_p$$

has been used to calculate the difference in enthalpy between the constant enthalpy curves of Fig. 3 here, and Fig. 8 of the first paper. $C$ varies so very slowly over the whole temperature range at 1 atm. pressure, that average values of $C$ for the temperature step are quite sufficient. It is not feasible to evaluate the integration constant so an arbitrary zero has been selected at 0° C. and 1 atm.

In Table 16 is given the value for the enthalpy of each curve to as low a temperature as the value of $C$ was available. The value of $C\Delta t$ for the same value of $\Delta T$ at 215 atm. varies over about $\pm$ 2%. These values of $\Delta T$ at 1 atm. are really the differences of considerably larger experimental values so that this treatment exaggerates the experimental errors. To lessen this erratic variation, the values were smoothed by plotting, being careful to keep the same total change in $h$.

It is evidently a routine matter to cross plot these $h$ = const. curves of Fig. 3 here and of Fig. 8 of the first paper, to give either the variation of $h$ with $t$ at constant $p$ (the usual "total heat diagram") or the variation of $h$ with $p$ at constant $t$. As no immediate use was to be made of them here, they are not given.

### 15. Rate of Change of Heat with Pressure, $\mu C = \left(\frac{dQ}{dp}\right)_h$.

Since the values of $\mu$ $C$ are of considerable use in thermodynamic calculations and are used later here, the data for the low temperature range are collected in Table 17, which is therefore the complement of Table XIV of the first paper.[1] The values are obtained by multiplying together the value of $\mu$ in °C/atm. from Table 13 and $C$ in cal./g.° C. from Table 15. To obtain these in C. G. S. mechanical units (cc./g.) they must be multiplied by

$$41.38 = \frac{4.188 \times 10^7}{13.59 \times 76 \times 980}$$

The values are negative in part of the field corresponding to the negative values of $\mu$. In the general neighborhood of the critical state $C$ varies rapidly and so here controls the variation of $\mu C$ but over the rest of the field $\mu$ varies the more rapidly. On account of the uncertainty in the values of $C$ below room temperature, the probable error in $\mu C$ is largest there.

### 16. *pv* Data for Air.

In order to make use of Equations 2 and 7 for the computation of $\alpha_p$ and $\eta$ it was necessary to look up the data on $pv$ as a function of pressure and temperature. The data divide naturally into two groups, one above room temperature and the other below.

For the region 0° to 200° C. and 0 to 100 atmospheres use was made of the data of Holborn and Schultze.[17] The data were plotted on a large scale as isothermals, $pv$ against $p$, and from these curves data were picked off for plotting isopiestics, $pv$ against $t$. This allowed of selecting the values of $pv$ and from this of the specific volume $v$, at the particular values of $p$ and $t$ used in the other tables. The values of $v$ are collected in Table 18. The precision is probably better than that required for the computation of $\alpha_p$.

The values of $\left(\frac{d(pv)}{dt}\right)_p$ and $\left(\frac{d(pv)}{dp}\right)_t$ required for use with Equation 14, are of course the slopes of these isopiestics and isothermals respectively. These slopes were consequently picked off by graphical means and smoothed by plotting and cross plotting. It was found necessary to interpolate for the 25° and 75° isothermal by interpolating the data for the slopes, since interpolating the original data led to quite inconsistent results for the slopes. The original data do not lead to very consistent curves, either on account of experimental error or because air has this character. The smoothing process was carried only far enough to smooth out chance errors in our treatment, but not far enough to interfere with the original character of the data. The data for the two coefficients are collected in Tables 19 and 20.

The low temperature $pv$ curves had to be built up from a rather fragmentary collection of data from different workers. The data used were (1) that by Penning as given in International Critical Tables, Vol. 3, p. 10, (2) the isothermal given by Koch [18] at −79.1° C., (3) the isothermal at 0° from Holborn and Schultze,[17] (4) the points given by Witkowski[19] of zero slope of the isothermals. The isothermals so built up were cross plotted as isopiestics to allow of interpolat-

ing for the particular isothermals desired in the tables. These gave the values of $pv$ which were used to obtain the specific volume data for the lower temperature range given in Table 18.

As before, these isothermals and the isopiestics plotted from them were used to obtain the values of the slopes $\left(\frac{d(pv)}{dp}\right)_t$ and $\left(\frac{d(pv)}{dt}\right)_p$ by graphical means. The resulting values were as before smoothed, but only to aid the graphical treatment, not to submerge the character of the data. Considerable extrapolation was necessary. The pressure coefficient is consequently apt to be in error, particularly at those values of $p$ and $t$ where the coefficient is small. On account of the data available the $-75°$ isothermal and the 60 atm. isopiestic are the most reliable, and therefore also their respective coefficients (slopes). The effect of the interpolation and extrapolation necessitated by the fragmentariness of the data is evident in Table 19 in the 20 atm. row. At a constant pressure of 20 atm., the temperature coefficient should surely decrease continuously with rising temperature, instead of erratically as in the table. Nevertheless, the actual value of this coefficient appears to be reliable to 3 to 5% or better. The pressure coefficient is not quite as good.

### 17. Coefficient of Volume Expansion $\alpha_p$.

Equation 2 above may be put in the form

$$\left[\frac{\mu C}{v} + 1\right]\frac{1}{T} = \frac{1}{v}\left(\frac{dv}{dT}\right)_p = \alpha_p \tag{10}$$

in which it is at once evident that $\frac{\mu C}{v}$ is proportional to the divergence of $\alpha_p$ from the reciprocal of $T$, and gives it as a measured difference. From which if

$$\frac{\mu C}{v} \gtreqless 0 \quad \text{then} \quad \alpha_p \gtreqless \frac{1}{T}$$

and as experimentally $\mu$ may be $\gtreqless 0$, it follows that $\alpha_p$ may be either larger or smaller than $\frac{1}{T}$. At the critical state both C and $\alpha_p$ become infinite.

At 1 atm $\frac{\mu C}{v}$ is small compared to unity; for example, at 0° C. it

is 0.0034, so that 1% error in $\frac{\mu C}{v}$ introduces only 0.0034% error in $\alpha_p$. The value of $\frac{1}{T_0}$ comes effectively from a coefficient measurement, but has a small $\mu C$ correction, so that the variations in the value of $\alpha_p$ at these low pressures can be evaluated from these $\mu C$ data with more precision than they can be measured directly.

As the pressure is increased $v$ decreases very rapidly, so that at 100 atm. $\mu C$ and $v$ are about the same size, and hence the error in $\alpha_p$ is only slightly reduced from that in $\frac{\mu C}{v}$. As the difficulty in a direct measurement at this pressure is great, possibly the computed value would be still the better.

$\alpha_p$ has been computed (Table 21) using Eq. 17, $\mu C$ in cal./g. atm. from Table 17, which is converted into cc./g. as described above and $v$ from Table 18. It should be noted that these values of $\alpha_p$ are not averages over a range in temperature but are the differential values at the particular temperature and pressure specified.

## 18. Free Expansion or Joule Coefficient $\eta = \left(\frac{dT}{dp}\right)_u$.

Equation (7) above may be used readily for computing $\eta$ and the values are detailed in Table 22. The necessary data for $C$ were picked from Table 15; for $\left(\frac{d(pv)}{dT}\right)_p$ from Table 19 in L./g. atm. and changed to cal./g. ° C. by multiplying by 24.17; for $\mu C$ from Table 17 and First Paper Table XIV; for $\left(\frac{d(pv)}{dp}\right)_t$ from Table 20 in L./g. atm. and changed to cal./g. atm. by multiplying by 24.17.

For the whole range the second term in the bracket runs about ⅓ of $C$, the two terms varying somewhat together. The last term on the right runs from about 5% of $\mu C$ at −75° C. and 140 atm. to 150% at + 200° C. and 100 atm: that is, in the range near the critical state where $C$ grows very rapidly $\mu C$ dominates, but where $\mu$ is small in the neighborhood of the inversion temperature $\mu C$ becomes relatively unimportant. Where $\mu C$ vanishes the second term is still strongly of account so that as far as can be inferred from this data $\eta$ does not go to zero. This is of course the behavior to be expected from the kinetic theory in which the force between the molecules does not

vanish except perhaps for very great separation, a case not even remotely estimable from the above data. In consequence of the relative sizes of the terms it appears that they all have material importance in fixing the value of $\eta$, and it is correspondingly difficult to estimate the precision with which $\eta$ is known.

Evidently from Eq. 4, $\eta \gtreqless \mu$ according as $\left(\frac{d(pv)}{dp}\right)_u \gtreqless 0$. If one attempts to estimate $\left(\frac{d(pv)}{dp}\right)_u$ from the isothermal case $\left(\frac{d(pv)}{dp}\right)_T$, there arises the effect on $(pv)$ of the temperature variation in the $(pv)_u$ case, which on account of the small variation of $(pv)_t$ may actually dominate. There are no measurements leading to a knowledge of the variation of $(pv)_u$, though it could be calculated from the data in this paper by using Eq. 4.

So far as I know there are no published experimental measurements of $\eta$. Joule's work led to no numerical values. It was tried in this laboratory by one of my students, E. V. Floyd, using air, and allowing it to expand from an inner vessel into the space between, which was previously evacuated. This made it possible to reduce the material sharing the change of temperature with the air, to less than 300 times the mass of the air. The interpretation of the experimental data is much complicated by the change of temperature of the two vessels' walls, due to their changes of stress. The serious mechanical difficulties in the construction of the vessel occupied most of the available year. The preliminary data obtained however was just what was expected but was neither elaborate enough nor sufficiently certain to justify separate publication. When opportunity offers the problem will be taken up again as it is decidedly advisable to check at least part of the data of Table 22 by direct experimental measurement.

Worthing[14] has calculated both $\mu$ and $\eta$, from Eq. 2 for $\mu$ and an equation which he derived by a cyclic argument for $\eta$. Both equations involve small differences in a way to magnify the error in the data. Table 23 shows the way his data compares with that in this paper. Considering the difficulties involved in his situation—none too trustworthy or abundant data, complex formula, involving small differences—the agreement is excellent.

H. Hausen[12] has also used his measurements of $\mu$ to calculate the numerical magnitude of a number of the physical properties of air, among which is the free expansion coefficient. His method of analysis is radically different from that used in this article, as he employs

with great skill mostly cyclic arguments referring directly to real or ideal experiments. For his calculation he also requires the $pv$ relations of air.

His values of $\eta$ are given only in the form of small curves, and he claims only 10% accuracy, on account of the exaggerated effect of small errors in the graphical and numerical treatment. For comparison with Table 22, his values of $\eta$ have been picked off these curves over the range of comparison only, and are given here as Table 22A. As will be observed, his values are almost uniformly larger than mine by at least 10%. The trends are quite similar—a small rise with pressure at low pressures, and a steady fall at higher pressures, as well as a fall with rising temperature when distinctly above the critical temperature.

19. ELASTIC COEFFICIENT $-\gamma = \frac{1}{v}\left(\frac{dv}{dp}\right)_t$ IN $(\text{ATM})^{-1}$.

Equation (9) may be readily rewritten as

$$-\gamma = \frac{1}{v}\left(\frac{dv}{dp}\right)_t = \eta\left[\frac{41.38C}{pv} - \alpha_p\right] - \frac{T\alpha_p}{p}$$

This has been used to calculate the values of $\gamma$ given in Table 24, using $\eta$ from Table 22 in °C/atm., $C$ from Table 15 in g.cal/° C, $v$ from Table 18 in cc/g., and $\alpha_p$ from Table 21 in $(°C.)^{-1}$.

Numerically, of the two terms within the brackets on the right, $\alpha_p$ is usually about one quarter of the first term, while the term $\eta\left[\frac{C41.38}{pv} - \alpha_p\right]$ makes a small correction, $0.5\% - 0.2\%$ for the low pressures to $50\% - 25\%$ for the higher pressures, on the term $\frac{T\alpha_p}{p}$.

If the gas obeys Boyle's law, then $\gamma$ becomes equal to 1/p. For comparison, the values of 1/p are given in the right hand column of Table 24. It will be observed that the tabulated values are in all cases quite close to the corresponding value of 1/p. Also these tabulated values fall slightly with rising temperature at all pressures, generally somewhat more rapidly at the lower temperatures, and generally rapidly enough that the irregularities do not obscure the drift. That is, at all the pressures shown the air is more compressible than the ideal gas at the lower temperatures and less compressible at the higher temperatures.

## 20. Constant Pressure Air Scale.

In the first paper[1] the Kelvin scale temperature of the ice point was calculated as 273.15° K., using the available values of the average coefficient between the ice point and the steam point, and the values of $\mu C$ for the same range. These corrections are now extended to the range covered by these experiments. The method used is that due to Buckingham,[20] which was used also by Hoxton.[21]

Eq. 2 above may be readily rewritten in the integral form[1]

$$\frac{v}{T} - \frac{v_0}{T_0} = \int_{T_0}^{T} \frac{C\mu dT}{T^2} \tag{11}$$

and this used to write the working equation

$$t_a - t = 0.7012\,\alpha t - TT_0\rho_0\,0.0413 \int_{T_0}^{T} \frac{\mu C}{T^2}\,dT \tag{12}$$

where $T_0$ is the ice point on the Kelvin scale already calculated from these data, and

$$T_0 = \frac{1}{\alpha} + 0.7012$$

where $\alpha = 0.0036708$ ($p = 760$ mm.). $T$ is the temperature on the Kelvin scale so that $t_a = T - T_0$ and $t$ is the temperature on the Centigrade air scale. $\rho = 1.293$ g/L at 760 mm. and 0° C.

To evaluate the integral use was again made of the relation

$$\mu C = \frac{A}{T} + B$$

which represents $uC$ quite accurately over moderate ranges of temperature, as shown in the first paper, for temperatures above room temperature. The integration was performed in steps to cover this range.

For the range below room temperature, $\mu C$ plotted against $1/T$ shows decidedly more curvature so the integration was carried out by determining $A$ and $B$ from the plot. The data on $\mu C$ for the low temperature range at 1 atm. are somewhat less reliable than at higher temperatures, as was shown by the lesser regularity of the values for the successive steps. It would appear also that the value of $\mu$ at 0° is somewhat low, as surmised also by O. C. Bridgman,[22] but re-examination of the data shows no present ground for altering the values. The data are given in Table 25, which gives also the data from Buckingham.[20]

These corrections apply to a thermometer using 760 mm. pressure, but it is possible to modify them without material error for a slightly different working pressure.

In Eq. (12) above

$$0.7012 = \frac{T_0(T_0 + 100)}{100\alpha}\rho_0 \int_{T_0}^{T_{100}} \frac{\mu C}{T^2}\, dT \tag{13}$$

so that $\rho_0$ is a factor in the right hand member of Eq. (12).

If the chosen new pressure is not sufficient to alter $\mu C$ materially, only $\rho_0$ among these other quantities is altered, so that

$$\frac{(t - t_a)^1}{(t - t_a)^{11}} = \frac{\rho_0{}^1}{\rho_0{}^{11}} = \frac{p_0{}^1}{p_0{}^{11}}$$

or the ratio of the densities or pressures will give with quite sufficient accuracy the ratio of the corrections.

21. Intrinsic Energy Variation with Volume. $\lambda = \left(\frac{du}{dv}\right)_T$.

In Eq. 1 above if one inserts the condition that the temperature remains constant, the result may be written

$$\lambda = \left(\frac{du}{dv}\right)_T = -T\left(\frac{dv}{dT}\right)_p \left(\frac{dp}{dv}\right)_T - p \tag{14}$$

$$= \frac{T\alpha_p}{\gamma} - p \tag{15}$$

where $\lambda$ is therefore a function of both $p$ and $t$.

This relation has been used to calculate $\lambda$ given in Table 26 using $\alpha_p$ from Table 19 in $(°C.)^{-1}$ and $\gamma$ from Table 24 in $(atm.)^{-1}$. $\lambda$ is therefore in atm. The two terms on the right of Equation 15 are numerically nearly alike at the low pressures (0.6% to 0.08% different) but this difference increases with pressure until in the extreme case the first term is more than twice the second (at $-75°$ C. and 140 atm.).

It will be noted that $\lambda$ falls with rising temperature at all pressures, by about a factor of 10 in the temperature range covered. Since one of the terms in the definition of an ideal gas is that $\lambda = 0$, this fall of $\lambda$ shows that the air is varying toward ideality rather rapidly over this temperature range.

On the other hand, $\lambda$ grows with extreme rapidity with pressure increase, at all temperatures, by a factor of about 10,000 for the 100 atm. rise. In terms of the definition of ideality, this means that at

the low pressures air is very close to the definition, but that it diverges very rapidly from it as the pressure is raised, seemingly more rapidly than it does from the $pv$ = const. term of the definition.

Such a table of values for $\lambda$ may evidently be used as a very convenient starting place in an attempt to estimate the law of force between molecules in the gas, as well as the actual forces. It is a very complicated problem and is unnecessarily difficult in this case on account of the presence of several molecular species, and of the complex nature of the molecules. A single atomed molecule (helium) of one species would be preferable.

## 22. Constant Volume Air Scale.

Eq. 14 above may be used to calculate the corrections of the (air) scale to the Kelvin scale as well as the Kelvin temperature of the ice point. Using the general relation

$$\left(\frac{dv}{dt}\right)_p \left(\frac{dp}{dv}\right)_t \left(\frac{dt}{dp}\right)_v = -1$$

Eq. (14) may be written

$$\lambda = T\left(\frac{dp}{dT}\right)_v - p$$

in which the similarity in form to Eq. (2) is evident. This may be used[20] to calculate the corrections for the constant volume air thermometer. By dividing through by $T^{-2}$ and rearranging

$$\frac{\lambda dT}{T^2} = d\left(\frac{p}{T}\right) \quad \text{or} \quad \frac{p}{T} - \frac{p_0}{T_0} = +\int_{T_0}^{T} - \lambda d\frac{1}{T} \qquad (16)$$

to which the condition $v$ = const. still adheres. Hence to integrate this, one must pick the values of $\lambda$ at the desired temperatures, each at such a pressure that the volume remains constant. These are then to be plotted against $T^{-1}$ and the area under the curve measured.

In Eq. 14 if $p$ be allowed to approach zero, then $\left(\frac{dp}{dv}\right)_t \doteq 0$ and $\therefore$ $\lambda \doteq 0$; therefore a plot of the curve, $\lambda$ against $p$ at constant temperature, starts from the origin. The actual plot shows that $\lambda$ grows very rapidly from the origin, the first part of the curve being only slightly curved, so that over a range of 0.5 to 1.6 atm. one may use $\lambda : p$ and determine the proportionality by the value of $\lambda$ at 1 atm.

As will appear from the size of the correction, 1% uncertainty in the values of $\lambda$ introduces about 1% in the correction, and this less than 0.01° in $T_0$. The range over which $p$ is to be used is from 0.5 to 1.6 atm., in which the general gas law will give proportionalities well within 1% uncertainty. Hence the pressures were calculated using $p : T$ for the series of temperatures from $-100$ to $+200$° C., using $p =$ 1 atm. at 0° C. Using these values of $p$ the corresponding values of $\lambda$ were calculated as indicated above. These $\lambda$'s were then plotted as a function of $T^{-1}$ and a smooth curve drawn through the points. There is considerably more irregularity among these points than in the points for $\mu$, so that the uncertainty here may run up to 5%. The curvature is not large, so that the integral of $\lambda d\frac{1}{T}$ may be taken assuming the curve a straight line over 25° C. steps from 0° C. to 100° C.; these integrals may be computed very simply by using

$$-\int_1^2 \lambda d\frac{1}{T} = \left(\frac{\lambda_1 + \lambda_2}{2}\right)\left(\frac{1}{T_1} - \frac{1}{T_2}\right)$$

which gives $23.09 \times 10^{-7}$ between the ice point and the boiling point.

The constant volume air scale is defined by the relation

$$p : t \quad v \text{ and } m \text{ constant}$$

and therefore

$$T = T_0 \frac{p}{p_0}$$

Let $T_0 =$ ice point, $T = T_0 + 100 =$ boiling point, $p = p_0(1 + \beta 100)$. Eq. (16) may then be written

$$\frac{p_0(1 + 100\beta)}{T_0 + 100} - \frac{p_0}{T_0} = 23.09 \times 10^{-7} \times \frac{p_0}{1}$$

The best available value of $\beta$ for air[20] is Chappuis', namely 0.00367442 per degree C. measured at $p_0 = \frac{1002}{760}$ atm. The $\lambda$ integral $(23.09 \times 10^{-7})$ is for $p_0 = 1$ atm., but since the individual values of $\lambda$ are proportional to the pressure, the integral is also. Hence, the relation may be written

$$T_0 = \frac{1}{\beta} + \frac{23.09 \times 10^{-7}\, T_0(T_0 + 100)}{100\beta}$$

in which the second member on the right is a small correction term in which $T_0 = 273$ is sufficient.

$$\therefore \quad T_0 = 272.152 + 0.640 = 272.79^\circ \text{ K}$$

When this is compared with $T_0 = 273.15$ calculated in the earlier paper, it is nearly 0.4° too small. To take up this discrepancy by changing $\lambda$ requires adding more than 50% to the above value of $\lambda$. The errors of the calculation save for the possible gross blunder, could not account for 50%. To put the burden on the value of $\beta$ would require an error of about 1 part in 700 which, in view of the care used, seems unlikely except for some unsuspected source of error. If one looks for this in the difference of gas absorption on the walls, the discrepancy appears large to account for this way, and on simple considerations would appear more likely to make $\beta$ relatively small compared to $\alpha$; that is, the resulting correction would be of the wrong sign.

It might be noted also that Buckingham[20] gives the corrections for the constant volume nitrogen thermometer as decidedly smaller than for the constant pressure case. If this applies also over the range $T = 0$ to $T =$ ice point, then the correction to $\frac{1}{\beta}$ should be smaller than the correction to $\frac{1}{\alpha}$. But the Chappius' values for $\alpha$ and $\beta$ require just the opposite; that is, the correction to $\frac{1}{\beta}$ must be the larger. As far as this is valid, it would be in agreement with the $\lambda$ result above and seem to throw the burden on Chappius' value of $\beta$.

In view of this discrepancy, it has not appeared profitable to calculate the corrections to the constant volume air scale, but they will be about $\frac{2}{3}$ those to the constant pressure scale.

## 23. Conclusion.

This finishes the work on air for the present, except that this data is being used to supply part of the material for an article on the liquifaction of air.

A list of the topics covered will be found on the first page.

I wish to acknowledge again, as in the first paper, the receipt of a grant from the Rumford Fund of the American Academy which was used for the purchase of the unglazed porcelain plugs use practically throughout the work, and contributing very materially to its success.

My acknowledgments are also due to my two effective helpers, Dr. J. H. Webb who except for his own modesty should have appeared as a co-author, and Mr. Harold Osterberg who helped in the computing and who is helping to gather the next experimental data. My thanks are due to both as energetic able partners in this work.

In the beginning of this attack on the Joule-Thomson problem years ago, air was selected as the working fluid for very obvious reasons —availability, cheapness, innocuousness of small leaks, etc. So that this attack is to be looked upon as a test out of the methods as well as an attempt to supply such data for air. Examination of the data taken as the work progressed will show a steady improvement as both the physical and mental situation came more and more under effective control. If the measurements were to be repeated, the numerical data could be improved very materially. Technically, air is a very important substance, but the need for high precision there is not great and Dr. Hausen's data as well as mine should suffice. Scientifically air is being increasingly neglected in favor of the pure gases, so that for example the data on $\alpha$ and $\beta$ used above are a good many years old.

Consequently the next move is to measure the pure gases. This involves using a low pressure reservoir as well as the high, and the use of a closed, tight system. This work has been pushed while the above computations have been in hand, so that the system is nearly ready for work. The Bureau of Mines is supplying helium as the first pure gas to be measured.

Department of Physics,
University of Wisconsin,
December 1929.

## List of References.

[1] Roebuck, J. R., Proc. Am. Acad. 60, 537, 1925.
[2] Sharples Solvents Corporation—Philadelphia.
[3] VanDusen, J. Am. Chem. Soc. 47, 326, 1925.
[4] Loomis and Walters, J. Am. Chem. Soc. 47, 2851, 1925.
[5] Henning, Temperature Messungen, F. Vieweg & Sohn, 1915.
[6] Kuenen & Clark, Leiden Communication No. 150.
[7] Dodge & Dunbar, Jour. Am. Chem. Soc. 49, 605, 1927.
[8] Knoblauch, Zeit. f. Tech. Phys. 5, 21, 1924.
[9] Witkowski, Phil. Mag. 41, 288, 1896.
[10] Jakob, M., Zeit. f. Tech. Phys. 4, 465, 1923.
[11] Callendar, H. L., Roy. Soc. Trans. A 212, 14, 1913.
[12] Hausen, H., Zeit. f. Tech. Phys. pp. 371 & 445, 1926. Also Wein & Harnes, Handbuch Experimental Physik Vol. 9, Part 1, Gasverflusingung by H. Lenz p. 87. Also Forschungsarbeiten herausgegeben von Verein Deutscher Ingenieure, Heft 274, "Der Thomson-Joul Effect und die Zustandgrossen der Luft" Vidi-verlag G. M. B. H. Berlin S. W. 19, 1926.
[13] Keesom, Comm. No. 88 Phys. Lab. Leiden.
[14] Worthing, A. G., Phys. Rev. 33, 217, 1911.
[15] Burnett, E. S., Phys. Rev. (2) 22, 590, 1923.
[16] Burnett, E. S., Bulletin of Univ. of Wisconsin Eng. Series Vol. IX, No. 6.
[17] Holborn & Schultze, Ann. d. Phy. 47, 1106, 1915.
[18] Koch, P. P., Ann. d. Phy. 27, 340, 1908.
[19] Witkowski, A. W., Phil. Mag. 41, 311, 1896.
[20] Buckingham, E., Bull. Bur. Sta. 3, 237, 1907.
[21] Hoxton, L. G., Phys. Rev. (2) 13, 438, 1919.
[22] Bridgman, O. C., Phys. Rev. (2), 34, 527, 1929.

TABLE 1.

A

| Plug No. | #51 Symbol ♌ $p$ | $-t$ |
|---|---|---|
| 1 | 73.5 | 21.56 |
| 2 | 91.2 | 17.69 |
| 3 | 109.7 | 14.02 |
| 4 | 128.1 | 10.80 |
| 5 | 140.7 | 8.67 |
| 6 | 154.4 | 6.51 |
| 7 | 168.4 | 4.63 |
| 8 | 180.9 | 3.35 |
| 9 | 215.8 | 0.0 |

B

| Plug No. | #41 Symbol ⊕ $p$ | $-t$ |
|---|---|---|
| 1 | 1.2 | 42.76 |
| 2 | 3.0 | 42.10 |
| 3 | 17.9 | 37.02 |
| 4 | 39.6 | 30.39 |
| 5 | 60.5 | 24.80 |
| 6 | 81.3 | 19.87 |
| 7 | 103.9 | 15.19 |
| 8 | 126.4 | 11.18 |
| 9 | 146.7 | 8.04 |
| 10 | 167.0 | 5.31 |
| 11 | 185.3 | 3.20 |
| 12 | 215.2 | 0.0 |

C

| Plug No. | #51 Symbol ♌ $p$ | $-t$ |
|---|---|---|
| 1 | 3.8 | 42.00 |
| 2 | 13.2 | 38.78 |
| 3 | 28.8 | 33.81 |
| 4 | 43.4 | 29.25 |
| 5 | 57.2 | 25.39 |
| 6 | 69.0 | 22.39 |
| 7 | 83.6 | 18.94 |
| 8 | 111.0 | 13.72 |

TABLE 2.

A

| Plug No. | #41 Symbol ⊕ $p$ | $-t$ |
|---|---|---|
| 1 | 1.3 | 76.90 |
| 2 | 2.9 | 76.23 |
| 3 | 10.3 | 72.94 |
| 4 | 26.2 | 66.06 |
| 5 | 46.2 | 58.38 |
| 6 | 66.0 | 51.86 |
| 7 | 88.4 | 45.57 |
| 8 | 112.6 | 39.86 |
| 9 | 132.7 | 35.92 |
| 10 | 154.0 | 32.36 |
| 11 | 172.4 | 29.67 |
| 12 | 193.5 | 27.15 |
| 13 | 215.2 | 25.20 |

B

| Plug No. | #35 Symbol ▽ $p$ | $-t$ |
|---|---|---|
| 1 | 44.3 | 58.49 |
| 2 | 64.0 | 53.30 |
| 3 | 86.1 | 46.23 |
| 4 | 112.3 | 40.09 |
| 5 | 134.9 | 35.73 |
| 6 | 156.8 | 32.12 |
| 7 | 177.6 | 29.27 |
| 8 | 213.6 | 25.01 |

C

| Plug No. | #49 Symbol ♉ $p$ | $-t$ |
|---|---|---|
| 1 | 80.6 | 47.86 |
| 2 | 100.1 | 42.73 |
| 3 | 123.9 | 37.63 |
| 4 | 139.9 | 34.63 |
| 5 | 147.0 | 33.39 |
| 6 | 159.1 | 31.66 |
| 7 | 171.9 | 29.82 |
| 8 | 213.6 | 25.01 |

D

| Plug No. | #49 Symbol ⊙ $p$ | $-t$ |
|---|---|---|
| 1 | 84.3 | 47.02 |
| 2 | 103.5 | 42.34 |
| 3 | 120.6 | 38.56 |
| 4 | 139.4 | 35.08 |
| 5 | 156.7 | 32.29 |
| 6 | 215.6 | 25.22 |

E

| Plug No. | #49 Symbol ⊡ $p$ | $-t$ |
|---|---|---|
| 1 | 1.8 | 76.76 |
| 2 | 10.8 | 72.80 |
| 3 | 26.3 | 66.07 |
| 4 | 39.5 | 60.90 |
| 5 | 52.9 | 56.11 |
| 6 | 67.3 | 51.46 |
| 7 | 81.9 | 47.12 |
| 8 | 110.4 | 40.40 |

TABLE 3.

A

| Plug No. | #35 $p$ | Symbol × $-t$ |
|---|---|---|
| 1 | 1.2 | 113.76 |
| 2 | 13.9 | 105.76 |
| 3 | 34.3 | 94.57 |
| 4 | 57.6 | 83.94 |
| 5 | 76.2 | 76.92 |
| 6 | 100.2 | 69.42 |
| 7 | 122.7 | 63.82 |
| 8 | 147.9 | 58.89 |
| 9 | 176.3 | 54.51 |
| 10 | 214.2 | 50.33 |

B

| Plug No. | #49 $p$ | Symbol ⊙ $-t$ |
|---|---|---|
| 1 | 131.9 | 61.94 |
| 2 | 146.1 | 59.23 |
| 3 | 162.4 | 56.51 |
| 4 | 169.6 | 55.48 |
| 5 | 184.4 | 53.50 |
| 6 | 213.6 | 50.33 |

C

| Plug No. | #49 $p$ | Symbol ♀ $-t$ |
|---|---|---|
| 1 | 89.0 | 72.83 |
| 2 | 105.2 | 68.24 |
| 3 | 120.2 | 64.48 |
| 4 | 135.0 | 61.30 |
| 5 | 213.6 | 50.33 |

D

| Plug No. | #49 $p$ | Symbol ♉ $-t$ |
|---|---|---|
| 1 | 1.0 | 113.58 |
| 2 | 1.3 | 113.20 |
| 3 | 20.2 | 101.56 |
| 4 | 46.6 | 88.67 |
| 5 | 64.4 | 80.94 |
| 6 | 215.2 | 50.86 |

TABLE 4.

A

| Plug No. | #35 $p$ | Symbol ⊙ $-t$ |
|---|---|---|
| 1 | 1.6 | 156.53 |
| 2 | 10.8 | 145.73 |
| 3 | 27.3 | 130.72 |
| 4 | 52.2 | 113.26 |
| 5 | 76.1 | 101.56 |
| 6 | 107.3 | 91.19 |
| 7 | 127.4 | 86.43 |
| 8 | 150.7 | 82.13 |
| 9 | 178.5 | 78.35 |
| 10 | 214.2 | 75.00 |

B

| Plug No. | #49 $p$ | Symbol ⊙ $-t$ |
|---|---|---|
| 1 | 127.8 | 86.54 |
| 2 | 140.6 | 84.02 |
| 3 | 157.4 | 81.59 |
| 4 | 163.4 | 80.27 |
| 5 | 178.3 | 78.37 |
| 6 | 213.6 | 75.00 |

C

| Plug No. | #49 $p$ | Symbol + $-t$ |
|---|---|---|
| 1 | 62.2 | 107.89 |
| 2 | 85.8 | 97.86 |
| 3 | 108.8 | 90.91 |
| 4 | 125.1 | 86.98 |
| 5 | 215.2 | 75.00 |

TABLE 5.

| | A | | | B | |
|---|---|---|---|---|---|
| Plug No. | #49 | Symbol ⊙ | Plug No. | #48 | Symbol ⊙ |
| | $p$ | $-t$ | | $p$ | $-t$ |
| 1 | 1.3 | 172.95 | 1 | 1.3 | 171.58 |
| 2 | 16.6 | 152.32 | 2 | 26.3 | 141.04 |
| 3 | 35.9 | 132.85 | 3 | 48.3 | 123.47 |
| 4 | 59.9 | 116.85 | 4 | 68.8 | 112.61 |
| 5 | 81.9 | 107.43 | 5 | 92.1 | 103.66 |
| 6 | 103.3 | 100.90 | 6 | 116.4 | 97.24 |
| 7 | 128.1 | 95.28 | 7 | 140.2 | 93.01 |
| 8 | 151.4 | 91.42 | 8 | 161.9 | 89.91 |
| 9 | 173.0 | 88.75 | 9 | 185.6 | 87.50 |
| 10 | 215.5 | 85.30 | 10 | 215.5 | 85.28 |

TABLE 6.

| | A | | | B | |
|---|---|---|---|---|---|
| Plug No. | #49 | Symbol ⊙ | Plug No. | #48 | Symbol ⊙ |
| | $p$ | $-t$ | | $p$ | $-t$ |
| 1 | 25.1 | 149.22 | 1 | 32.5 | 142.45 |
| 2 | 32.7 | 141.80 | 2 | 41.8 | 134.66 |
| 3 | 39.8 | 135.72 | 3 | 69.8 | 118.43 |
| 4 | 54.9 | 125.45 | 4 | 98.9 | 109.10 |
| 5 | 77.5 | 115.43 | 5 | 126.9 | 103.19 |
| 6 | 100.4 | 108.60 | 6 | 151.4 | 99.77 |
| 7 | 123.3 | 103.90 | 7 | 175.3 | 97.39 |
| 8 | 146.3 | 100.47 | 8 | 215.5 | 94.87 |
| 9 | 169.9 | 97.88 | | | |
| 10 | 215.5 | 94.87 | | | |

TABLE 7.

| | A | | | B | |
|---|---|---|---|---|---|
| Plug No. | #49 | Symbol + | Plug No. | #48 | Symbol ⊙ |
| | $p$ | $-t$ | | $p$ | $-t$ |
| 1 | 7.9 | 169.20 | 1 | 39.6 | 137.41 |
| 2 | 18.0 | 155.58 | 2 | 46.6 | 132.22 |
| 3 | 33.3 | 143.06 | 3 | 57.2 | 126.38 |
| 4 | 51.7 | 129.74 | 4 | 82.3 | 116.69 |
| 5 | 69.8 | 121.24 | 5 | 105.3 | 110.92 |
| 6 | 86.4 | 115.73 | 6 | 128.8 | 106.74 |
| 7 | 101.8 | 111.76 | 7 | 152.3 | 103.85 |
| 8 | 119.3 | 108.44 | 8 | 175.4 | 101.77 |
| 9 | 136.8 | 105.80 | 9 | 215.5 | 99.62 |
| 10 | 153.1 | 103.96 | | | |
| 11 | 169.6 | 102.43 | | | |
| 12 | 215.5 | 99.80 | | | |

TABLE 8.

| A | | | B | | |
|---|---|---|---|---|---|
| Plug #49 | | Symbol ☉ | Plug #48 | | Symbol ☌ |
| No. | $p$ | $-t$ | No. | $p$ | $-t$ |
| 1 | 33.0 | 144.16 | 1 | 37.3 | 141.26 |
| 2 | 39.4 | 138.84 | 2 | 41.1 | 138.18 |
| 3 | 46.0 | 134.66 | 3 | 50.8 | 131.98 |
| 4 | 52.8 | 130.18 | 4 | 61.3 | 126.83 |
| 5 | 70.2 | 123.35 | 5 | 87.1 | 118.19 |
| 6 | 95.3 | 116.25 | 6 | 114.9 | 112.54 |
| 7 | 118.2 | 112.12 | 7 | 144.7 | 108.76 |
| 8 | 141.2 | 109.09 | 8 | 175.1 | 106.23 |
| 9 | 163.8 | 107.07 | 9 | 215.5 | 104.38 |
| 10 | 215.5 | 104.38 | | | |

TABLE 9.

| A | | | B | | |
|---|---|---|---|---|---|
| Plug #49 | | Symbol △ | Plug #48 | | Symbol ☌ |
| No. | $p$ | $-t$ | No. | $p$ | $-t$ |
| 1 | 23.0 | 151.76 | 1 | 38.3 | 140.52 |
| 2 | 34.4 | 143.42 | 2 | 43.1 | 137.52 |
| 3 | 39.8 | 139.96 | 3 | 51.9 | 132.58 |
| 4 | 44.4 | 136.99 | 4 | 61.2 | 128.67 |
| 5 | 49.9 | 133.67 | 5 | 86.4 | 121.02 |
| 6 | 60.7 | 128.89 | 6 | 114.8 | 116.02 |
| 7 | 81.0 | 122.41 | 7 | 143.2 | 112.78 |
| 8 | 102.0 | 118.09 | 8 | 175.4 | 110.58 |
| 9 | 124.3 | 114.81 | 9 | 215.5 | 109.17 |
| 10 | 146.9 | 112.50 | | | |
| 11 | 163.6 | 111.35 | | | |
| 12 | 215.5 | 109.17 | | | |

TABLE 10.

| A | | | B | | |
|---|---|---|---|---|---|
| Plug #49 | | Symbol ⊙ | Plug #48 | | Symbol + |
| No. | $p$ | $-t$ | No. | $p$ | $-t$ |
| 1 | 25.6 | 149.37 | 1 | 47.6 | 136.18 |
| 2 | 38.5 | 140.81 | 2 | 73.1 | 128.66 |
| 3 | 50.1 | 135.36 | 3 | 96.8 | 124.95 |
| 4 | 66.1 | 130.45 | 4 | 124.9 | 122.02 |
| 5 | 90.1 | 125.40 | 5 | 148.5 | 120.42 |
| 6 | 112.9 | 123.08 | 6 | 174.5 | 119.25 |
| 7 | 136.1 | 121.12 | 7 | 215.5 | 118.60 |
| 8 | 157.9 | 119.88 | | | |
| 9 | 215.5 | 118.60 | | | |

TABLE 11.

A

| Plug No. | #48 $p$ | Symbol ⊙ $-t$ |
|---|---|---|
| 1 | 23.2 | 152.40 |
| 2 | 32.4 | 145.84 |
| 3 | 38.2 | 143.59 |
| 4 | 48.7 | 141.72 |
| 5 | 60.0 | 140.33 |
| 6 | 82.2 | 138.16 |
| 7 | 105.6 | 136.75 |
| 8 | 127.1 | 135.86 |
| 9 | 151.1 | 135.28 |
| 10 | 174.3 | 134.97 |
| 11 | 215.5 | 135.24 |

TABLE 12.

| Plug No. | #48 $p$ | Symbol ♀ $-t$ |
|---|---|---|
| 1 | 15.6 | 160.86 |
| 2 | 21.7 | 154.34 |
| 3 | 26.8 | 151.30 |
| 4 | 38.5 | 150.75 |
| 5 | 59.9 | 149.51 |
| 6 | 84.4 | 148.59 |
| 7 | 107.7 | 148.15 |
| 8 | 130.4 | 147.78 |
| 9 | 152.7 | 147.75 |
| 10 | 174.7 | 148.15 |
| 11 | 215.5 | 149.28 |

TABLE 13.

$\mu$ (low temps.).

| $P$ | −150° C. | −140° C. | −120° C. | −100° C. | −75° C. | −50° C. | −25° C. |
|---|---|---|---|---|---|---|---|
| 1 | | .9510 | .707 | .5750 | .4620 | .3755 | .3160 |
| 20 | | .9750 | .705 | .5535 | .4380 | .3565 | .2965 |
| 40 | +.0620 | .5700 | .672 | .5210 | .4105 | .3325 | .2750 |
| 60 | +.0440 | .1105 | .522 | .4700 | .3765 | .3080 | .2540 |
| 80 | +.0315 | .6800 | .294 | .3870 | .3330 | .2785 | .2330 |
| 100 | +.0190 | .0435 | .1650 | .2845 | .2870 | .2470 | .2115 |
| 120 | +.0070 | .0285 | .1015 | .1990 | .2705 | .2135 | .1865 |
| 140 | −.0030 | .0155 | .0845 | .1415 | .1960 | .1815 | .1640 |
| 160 | −.0125 | +.0020 | .0460 | .1030 | .1475 | .1550 | .1435 |
| 180 | −.0215 | −.0080 | .0285 | .0745 | .1165 | .1305 | .1250 |
| 200 | −.0280 | −.0175 | +.0130 | .0490 | .0920 | .1100 | .1075 |
| 220 | −.0385 | −.0280 | −.0150 | .0310 | .0685 | .0935 | .0975 |

TABLE 14.

$\mu$ FROM TABLE 13 IN ROMAN TYPE.
$\mu$ FROM HAUSEN'S WORK IN ITALIC TYPE.

| $P$ | −150° C. | −140° C. | −120° C. | −100° C. | −75° C. | −50° C. | −25° C. | 0° C. | +25° C. |
|---|---|---|---|---|---|---|---|---|---|
| 1 | | .971 | .707 | .575 | .462 | .376 | .316 | .266 | .227 |
| *0* | | *1.028* | *.796* | *.642* | *.501* | *.399* | *.327* | *.269* | *.224* |
| 100 | +.019 | .044 | .165 | .285 | .287 | .247 | .215 | .178 | .152 |
| *100* | −.006 | *.015* | *.164* | *.244* | *.166* | *.168* | *.127* | *.086* | *.055* |
| 200 | −.028 | −.018 | −.013 | +.049 | .092 | .110 | .108 | .084 | .073 |
| *200* | −.035 | −.030 | −.007 | +.028 | *.075* | *.100* | *.110* | *.095* | *.088* |

TABLE 15.

$Cp$ AS FUNCTION OF $p$ AND $t$ g. cal/°C.

| $P$ | −100° C. | −75° C. | −50° C. | −25° C. | 0° C. | +25° C. | +50° C. | +75° C. | +100° C. | +150° C. | +200° C. | +250° C. | +280° C. |
|---|---|---|---|---|---|---|---|---|---|---|---|---|---|
| 1 | .2385 | .2390 | .2394 | .2399 | .2405 | .2410 | .2415 | .2419 | .2424 | .2434 | .2443 | .2453 | .2458 |
| 20 | .2757 | .2630 | .2556 | .2514 | .2492 | .2487 | .2480 | .2475 | .2470 | .2466 | .2463 | .2468 | .2471 |
| 60 | | .3184 | .2883 | .2744 | .2656 | .2627 | .2603 | .2581 | .2562 | .2532 | .2512 | .2500 | .2492 |
| 100 | | .3940 | .3264 | .2979 | .2838 | .2760 | .2717 | .2681 | .2650 | .2602 | .2565 | .2536 | .2519 |
| 140 | | .4427 | .3561 | .3171 | .2985 | .2873 | .2816 | .2767 | .2725 | .2658 | .2607 | .2566 | .2544 |
| 180 | | | .3747 | .3317 | .3093 | .2960 | .2898 | .2840 | .2790 | .2707 | .2644 | .2596 | .2569 |
| 220 | | | .3780 | .3393 | .3183 | .3020 | .2956 | .2893 | .2838 | .2748 | .2678 | .2622 | .2593 |

TABLE 16.

Enthalpy, $h = u + pv$, g. cal.

| Curve | $h$ |
|---|---|
| 280 | 78.53 |
| 250 | 70.68 |
| 200 | 57.41 |
| 150 | 43.83 |
| 100 | 29.87 |
| 75 | 22.70 |
| 50 | 15.36 |
| 25 | 7.82 |
| 0 | 0.00 |
| −25 | −8.22 |
| −50 | −17.07 |
| −75 | −27.07 |
| −85 | −31.57 |

TABLE 17

$\mu C$.

From Tables 13 and 14 g. cal/g. atm.

| $P$ | −100° C. | −75° C. | −50° C. | −25° C. | 0° C. |
|---|---|---|---|---|---|
| 1 | .137 | .1104 | .0899 | .0758 | .0640 |
| 20 | .153 | .1152 | .0911 | .0745 | .0622 |
| 60 | | .1199 | .0888 | .0697 | .0569 |
| 100 | | .1131 | .0806 | .0630 | .0506 |
| 140 | | .0868 | .0646 | .0520 | .0431 |
| 180 | | | .0489 | .0415 | .0348 |
| 220 | | | .0353 | .0331 | .0258 |

TABLE 18.

SPECIFIC VOLUMES IN $\left(\frac{cc}{g}\right) \times 10^{-3}$.

| $P$(atm.) | −100° C. | −75° C. | −50° C. | −25° C. | 0 | +25° C. | +50° C. | +75° C. | +100° C. | +150° C. | +200° C. |
|---|---|---|---|---|---|---|---|---|---|---|---|
| 1 | .5014 | .5578 | .6212 | .7007 | .7735 | .8439 | .9150 | .9862 | 1.0574 | 1.1989 | 1.3408 |
| 20 | .02283 | .02611 | .03017 | .03419 | .03859 | .0420 | .04567 | .04927 | .05298 | .06025 | .06745 |
| 60 | | .00805 | .00959 | .01114 | .01253 | .01394 | .01524 | .01655 | .01779 | .02034 | .02282 |
| 100 | | .00450 | .00561 | .00657 | .00751 | .00837 | .00920 | .01005 | .01083 | .01237 | .01392 |
| 140 | | .00318 | .00395 | .00470 | | | | | | | |
| 180 | | | .00316 | .00371 | | | | | | | |

TABLE 19.

$\left(\frac{d(pv)}{dt}\right)_p \times 10^3$ $\quad v$ is in $L/g$, $p$ in atm., $t$ in °C.

| $P$ | −100° C. | −75° C. | −50° C. | −25° C. | 0° C. | +25° C. | +50° C. | +75° C. | +100° C. | +150° C. | +200° C. |
|---|---|---|---|---|---|---|---|---|---|---|---|
| 1 | 2.835 | 2.835 | 2.835 | 2.835 | 2.835 | 2.835 | 2.835 | 2.835 | 2.835 | 2.835 | 2.835 |
| 20 | 3.196 | 3.039 | 3.094 | 3.094 | 2.943 | 2.942 | 2.938 | 2.925 | 2.914 | 2.908 | 2.908 |
| 60 | | 4.093 | 3.551 | 3.318 | 3.117 | 3.115 | 3.099 | 3.068 | 3.023 | 2.983 | 2.978 |
| 100 | | 4.720 | 4.124 | 3.713 | 3.512 | 3.441 | 3.344 | 3.210 | 3.119 | 3.067 | 3.054 |
| 140 | | 4.880 | 4.200 | 3.838 | | | | | | | |
| 180 | | | 4.038 | 3.814 | | | | | | | |

TABLE 20.

$$+\left(\frac{d(pv)}{dp}\right)_t \times 10^4 \qquad v \text{ IN } L/g, \text{ AND } p \text{ IN ATM.}$$

| $P$ | −100° C. | −75° C. | −50° C. | −25° C. | 0° C. | +25° C. | +50° C. | +75° C. | +100° C. | +150° C. | +200° C. |
|---|---|---|---|---|---|---|---|---|---|---|---|
| 1 | −24.74 | −14.12 | −11.36 | −8.498 | −4.33 | −2.57 | −1.04 | 0.008 | 0.92 | 2.70 | 4.21 |
| 20 | −23.52 | −13.31 | −9.292 | −6.653 | −3.73 | −1.90 | −0.37 | 0.71 | 1.66 | 3.31 | 4.52 |
| 60 | | −10.83 | −5.570 | −4.023 | −1.91 | −0.28 | +1.07 | 2.16 | 3.08 | 4.33 | 5.18 |
| 100 | | −5.106 | −2.166 | −1.248 | +0.62 | +1.67 | 2.60 | 3.47 | 4.25 | 4.95 | 5.85 |
| 140 | | +1.778 | +1.161 | +1.161 | | | | | | | |
| 180 | | | +4.251 | +3.482 | | | | | | | |

TABLE 21.

$\alpha_p \times 10^3$ (per °C.)

| $P$(atm.) | −100° C. | −75° C. | −50° C. | −25° C. | 0° C. | +25° C. | +50° C. | +75° C. | +100° C. | +150° C. | +200° C. |
|---|---|---|---|---|---|---|---|---|---|---|---|
| 1 | 5.84068 | 5.08804 | 4.50814 | 4.04838 | 3.67168 | 3.36301 | 3.10091 | 2.87694 | 2.68326 | 2.36506 | 2.11399 |
| 20 | 7.374 | 5.967 | 5.041 | 4.393 | 3.905 | 3.528 | 3.218 | 2.961 | 2.743 | 2.397 | 2.131 |
| 60 | | 8.161 | 6.198 | 5.073 | 4.348 | 3.828 | 3.428 | 3.108 | 2.848 | 2.450 | 2.157 |
| 100 | | 10.30 | 7.298 | 5.631 | 4.681 | 4.048 | 3.577 | 3.213 | 2.921 | 2.484 | 2.169 |
| 140 | | 10.75 | 7.514 | 6.051 | | | | | | | |
| 180 | | | 7.351 | 5.895 | | | | | | | |

TABLE 22.

$$\eta = \left(\frac{dT}{dp}\right)_u \text{ in °C./atm.}$$

| $P$ | −100° C. | −75° C. | −50° C. | −25° C. | 0° C. | +25° C. | +50° C. | +75° C. | +100° C. | +150° C. | +200° C. |
|---|---|---|---|---|---|---|---|---|---|---|---|
| 1 | .455 | .448 | .365 | .322 | .311 | .281 | .249 | .220 | .198 | .172 | .145 |
| 20 | .482 | .438 | .379 | .331 | .299 | .270 | .244 | .218 | .197 | .165 | .140 |
| 60 | | .427 | .372 | .309 | .275 | .242 | .228 | .207 | .188 | .156 | .133 |
| 100 | | .360 | .301 | .288 | .244 | .219 | .214 | .195 | .179 | .146 | .126 |
| 140 | | .280 | .265 | .244 | | | | | | | |
| 180 | | | .214 | .208 | | | | | | | |

TABLE 22A.

from Hausen's work.

| $P$ | −73.2° C. | −23.2° C. | +26.8° C. |
|---|---|---|---|
| 1 | .505 | .36 | .27 |
| 20 | .53 | .36 | .27 |
| 60 | .515 | .345 | .26 |
| 100 | .425 | .325 | .25 |
| 140 | .34 | | |

TABLE 23.

$\mu$ and $\eta$ Comparison with Worthing.

| | $\mu$ | | | | $\eta$ | | | |
|---|---|---|---|---|---|---|---|---|
| | $W$ | $R$ | $W$ | $R$ | $W$ | $R$ | $W$ | $R$ |
| $P$ | −79.3° C. | −75° C. | 0° C. | 0° C. | −79.3° C. | −75° C. | 0° C. | 0° C. |
| 1 | .230 | .462 | | .240 | | .448 | | .311 |
| 20 | .464 | .438 | .226 | .249 | .476 | .438 | .259 | .299 |
| 60 | .424 | .377 | .212 | .266 | .474 | .427 | .278 | .275 |
| 100 | .293 | .287 | .186 | .280 | .368 | .360 | .270 | .244 |
| 140 | .214 | .196 | .130 | | .296 | .280 | .233 | |

TABLE 24.

ELASTIC COEFFICIENT, $-\gamma = \frac{1}{v}\left(\frac{dv}{dp}\right)_t$ (ATM.)$^{-1}$.

| $P$ | −100° C. | −75° C | −50° C. | −25° C. | 0° C. | +25° C. | +50° C. | +75° C. | +100° C. | +150° C. | +200° C. | $1/p$ |
|---|---|---|---|---|---|---|---|---|---|---|---|---|
| 1 | 1.0051 | 1.0025 | 1.00179 | 1.00125 | 1.00014 | 1.00030 | 1.00014 | 1 000 | 1.00018 | 0.99971 | 0.99944 | 1.0000 |
| 20 | 0.05534 | 0.05261 | 0.05151 | 0.05093 | 0.05050 | 0.05024 | 0.05004 | 0.049 | 0.04982 | 0.04975 | 0.04965 | 0.05000 |
| 60 | | 0.01878 | 0.01764 | 0.01730 | 0.01697 | 0.01680 | 0.01656 | 0.0164 | 0.01638 | 0.01632 | 0.01629 | 0.01667 |
| 100 | | 0.01106 | 0.01123 | 0.01020 | 0.01011 | 0.00996 | 0.00982 | 0.00966 | 0.00961 | 0.00960 | 0.009575 | 0.01000 |
| 140 | | 0.006797 | 0.006907 | 0.00734 | | | | | | | | 0.007143 |
| 180 | | | 0.004853 | | | | | | | | | 0.005555 |

TABLE 25.

CORRECTIONS TO CONSTANT PRESSURE AIR SCALE TO BE ADDED TO EXPERIMENTAL DATA TO GIVE ° KELVIN.

| $t$° C. | $p$ = 760 Roebuck | $p$ = 1000 Roebuck | $p$ = 1000 Buckingham |
|---|---|---|---|
| +280 | .202 | .266 | |
| 250 | .161 | .212 | |
| 225 | .127 | .167 | |
| 200 | .0959 | .126 | .105 |
| 175 | .0668 | .0879 | |
| 150 | .0406 | .0534 | |
| 125 | .0181 | .0238 | |
| 100 | .0000 | .0000 | .0000 |
| 75 | −.0128 | −.0168 | −.0151 |
| 50 | −.0185 | −.0243 | −.0209 |
| +25 | −.0149 | −.0196 | −.0158 |
| 0 | .0000 | .0000 | .0000 |
| −25 | .0289 | .0380 | |
| −50 | .0971 | .128 | |
| −75 | .154 | .203 | |
| −100 | .273 | .359 | 0.326 |
| | Air | Air | Nitrogen |

TABLE 26

$$\lambda = \left(\frac{du}{dv}\right)_t \text{ IN ATM.}$$

| $P$ | −100° C. | −75° C. | −50° C. | −25° C. | 0° C. | +25° C. | +50° C. | +75° C. | +100° C. | +150° C. | +200° C. |
|---|---|---|---|---|---|---|---|---|---|---|---|
| 1 | .006182 | .005681 | .004194 | .003351 | .002779 | .002381 | .001919 | .001597 | .001078 | .001066 | .000795 |
| 20 | 3.072 | 2.474 | 1.838 | 1.404 | 1.120 | .9339 | .7239 | .6505 | .5449 | .3878 | .3078 |
| 60 | | 26.11 | 18.41 | 12.77 | 9.985 | 7.936 | 6.894 | 5.778 | 4.879 | 3.524 | 2.651 |
| 100 | | 84.53 | 45.02 | 36.99 | 26.05 | 21.09 | 17.71 | 15.79 | 13.42 | 9.456 | 7.181 |
| 140 | | 173.4 | 102.8 | 64.57 | | | | | | | |
| 180 | | | 158.0 | | | | | | | | |